ISSN 1063-7710, Acoustical Physics, 2021, Vol. 67, No. 3, pp. 320–328. © Pleiades Publishing, Ltd., 2021.
Russian Text © The Author(s), 2021, published in Akusticheskii Zhurnal, 2021, Vol. 67, No. 3, pp. 328–337.

ACOUSTIC SIGNALS PROCESSING. COMPUTER SIMULATION

Broadband Vibrometry of a Two-Dimensional Ultrasound Array Using Transient Acoustic Holography

S. A. Tsysar[a], *, D. A. Nikolaev[a], and O. A. Sapozhnikov[a]

[a] *Moscow State University, Faculty of Physics, Moscow, 119991 Russia*

**e-mail: sergey@acs366.phys.msu.ru*

Received May 2, 2020; revised January 25, 2021; accepted February 2, 2021

Abstract—The article presents the results of experimental determination of the structure of surface vibrations of a two-dimensional phased ultrasound probe using transient acoustic holography in the frequency range from 0.1 to 10 MHz. It is shown that this method makes it possible to detect individual elements operating with parameter deviations from the nominal values, including inactive ones. A comparison is made with the results of echo pulse measurements for each element, as well as measurements of the electric capacitance of the elements.

Keywords: acoustic holography, two-dimensional arrays, characterization of sources, calibration

DOI: 10.1134/S1063771021030131

INTRODUCTION

Multielement ultrasound (US) arrays are widely used in medical diagnostics and nondestructive testing. In most modern ultrasound scanners, one-dimensional (linear) ultrasound arrays are used, which, due to special phasing of signals from various elements, allow echo pulse visualization in a two-dimensional area—a flat site perpendicular to the array elements. Improvement of obtained images in comparison with the simplest DAS (*delay and sum*) construction method is achieved with new signal processing algorithms [1, 2] and recognition methods [3, 4]. In recent years there has been a trend of using two-dimensional arrays, which can significantly improve ultrasound visualization or the therapeutic application accuracy by not only covering a three-dimensional area, but also by more efficient compensation of aberrations when ultrasound methods are used in inhomogeneous media [5].

When using such arrays, the elements are usually considered ideal, which is often a very rough approximation. In reality, it is important to be able to control the state of separate elements, as well as their ability to emit and receive signals in the required frequency range. It is also desirable to estimate the state of the protective and matching layers on the emitting surface, the quality of electric contacts between piezoelectric elements and their supply wires, etc. When determining the nature of the emitted ultrasound field, developers sometimes limit themselves to a set of electric characteristics of elements using various approximations (for example, assumptions about the piston nature of element-surface oscillations). For a number of applications, this may be unacceptable in level of accuracy of the predicted field due to a number of defects and the inappropriateness of the approximations used [6]. The nature of source-surface oscillations can be determined by well-known methods, e.g., laser vibrometry [7] or schlieren visualization [8]. However, both of these methods cannot directly obtain the quantitative field distribution in a liquid working medium. The first method works in air, while acoustooptic interaction occurs in a liquid, which introduces significant interference [9, 10]. The second method makes it possible to simply obtain a qualitative picture of the ultrasound beam in a transparent fluid, but to obtain quantitative distributions, it is necessary to use a complex and high-precision tomography scheme. For a quantitative characterization of the radiated pulsed field, this study proposes transient acoustic holography [11].

In a broad sense, holography is the recording of complete information about a wave (holograms). In the case of a harmonic wave, not only the amplitude, but also the phase of the wave is recorded. According to the general properties of the solution to the wave equation, it is sufficient to make such a recording on some surface surrounding the visualized object. For acoustic waves, several holography options have been proposed and implemented in analogy with the optical recording principle [12–14]. Later it became clear that in acoustics it is possible to avoid the use of interference with an auxiliary reference beam, since, due to the relatively low signal frequency, it is quite easy to directly record the amplitude and phase of the wave at each point of the measurement surface, then recreate the original field numerically. Moreover, in the case of nonsinusoidal signals, it is possible to record the full

temporal waveform of signals at points on a specified surface. Such an approach was developed in [8, 11, 15–17] for the case of megahertz-range ultrasound waves propagating in fluids. The essence of the method is numerical calculation of the vibration velocity of the transducer surface based on the experimentally measured acoustic pressure distribution on a certain surface in front of the source. Mathematically, the problem is reduced to solving the inverse problem of finding the unknown field values at points of the source surface based on the known field values at points of a certain area of the surface in front of the source (hologram).

To date, several different acoustic holography versions have been proposed. One effective way to convert the wave field from plane to plane is the angular (spatial) spectrum method, which is used both for calculating the propagation of acoustic fields from plane sources [18, 19] and for backward recalculation [20], i.e., for holographic reconstruction by backpropagation. The angular spectrum method can be generalized to the case of cylindrical or spherical sources [21, 22]. A large number of publications are devoted to near-field acoustic holography, which is characterized by recording of a hologram at a relatively close distance from the source, on the order of the wavelength. This holography version was significantly developed in air acoustics, where it is already used to find the velocity or pressure distributions on vibrating surfaces of various devices. In this case, inhomogeneous waves are taken into account, which, as is known, carry information about small-scale details of the field at the source [23].

In this study, the method of transient acoustic holography is proposed and tested to determine the sensitivity of elements to radiation and the correspondence between the element and channel number of the ultrasound system. In the experiment, a 384-element ultrasound array with a center frequency of 2 MHz (Medelkom, Lithuania) was investigated. When calibrated in the 0.1–10 MHz frequency band, it was demonstrated that the proposed method has a high spatiotemporal resolution, which makes it possible to visualize the vibrations of individual elements and detect defects on the surface of the source.

THEORETICAL CONSIDERATION OF THE METHOD

In most ultrasound applications in medicine and nondestructive testing, the transducer dimensions are much larger than the wavelength, and the studied areas of the medium are at a distance much greater than the wavelength from the source; therefore, it is not necessary to take into account evanescent waves, in contrast to a number of holographic problems of hydroacoustics in the kilohertz range [12, 13]. The developed acoustic holography option is based on the principle of wavefront reversal, based on invariance of the wave equation in a nonabsorbing medium with respect to the time reversal operation [24]. To carry out forward or backward propagation, in some cases, it is convenient to use the Rayleigh integral method, which is especially convenient when studying nonplanar radiating surfaces vibrating according to a harmonic law [15]. Due to the linearity of the problem, it can easily be generalized to the case of nonstationary (in particular, pulsed) sources [17]. In this case, at each point of the hologram, not the amplitude and phase of the signal are recorded (as is done in the study of monochromatic sources), but the full waveform. This approach, as already noted, is valid when studying vibrations of the surface of a source and/or a measurement surface with a nonplanar shape, e.g., focusing [16].

When the surface of the scanned area (hologram) and the surface of the source are plane-parallel, faster calculation is possible using the angular spectrum method. Note, however, that the speed of calculations is usually not a problem, so the choice of a particular method (Rayleigh integral or angular spectrum) is not critical. For definiteness, let us formulate the analytical regularities of forward and backward propagation of the ultrasound pressure field, which varies with time according to an anharmonic law, using Fourier transform. Let us consider a plane $z = 0$ located directly at the surface of a planar ultrasound source in water. The acoustic pressure distribution $p(x, y, z = 0, t)$ in this plane is determined by the nature of vibrations of the source surface, which is unknown. Due to the linearity of the problem, it is convenient to consider the propagation of each harmonic component of the signal $S(x, y, z, \omega)$ independently of others. The spatial structure of the field of each harmonic is the dependence of the actual amplitude and phase of this harmonic on the coordinates, which can be conveniently reduced to the spatial dependence of the complex amplitude, considering the function $S(x, y, z, \omega)$ to be complex. Within the framework of the angular spectrum method, this dependence can be reduced to $P(k_x, k_y, z, \omega)$ by moving from spatial coordinates (x, y, z) to mixed (k_x, k_y, z) using the 2D spatial Fourier transform:

$$P(k_x, k_y, z, \omega) = \int_{-\infty}^{\infty}\int S(x, y, z, \omega) e^{-ik_x x - ik_y y} dxdy, \quad (1)$$

where

$$S(x, y, z, \omega) = \int_{-\infty}^{\infty} p(x, y, z, t) e^{i\omega t} dt. \quad (2)$$

Here k_x, k_y are the projections of the wave vector $\mathbf{k}(\omega)$ for each harmonic component on the axis x and y, respectively. The z axis corresponds to the main direction of propagation of the ultrasound field.

Using the introduced notation, it is not difficult using the initial field on the plane $z = 0$ to express the angular spectrum of the harmonic field component on a plane far from the source at a distance z_H taking into account the acquired phase incursion $k_z z_H = \sqrt{k^2 - k_x^2 - k_y^2} z_H$ where $k = k(\omega) = \omega/c(\omega)$ is the wavenumber and c is the sound speed at a given frequency in the medium (for the considered case—in water):

$$P(k_x, k_y, z_H, \omega) = P(k_x, k_y, 0, \omega) G(k_x, k_y, z_H, \omega), \quad (3)$$

where

$$G(k_x, k_y, z_H, \omega) = e^{i\sqrt{\frac{\omega^2}{c^2} - k_x^2 - k_y^2} z_H}. \quad (4)$$

Thus, the angular spectra of the acoustic pressure field on parallel planes z are related by propagator G, which makes it easy to recalculate the field from one plane to another. In this case, the obtained expressions immediately make it possible to solve the inverse problem in the classical formulation of holography: for a known (from measurements) field on the hologram plane $z = z_H$, to find the field at the source. Indeed, multiplying the right- and left-hand sides of expression (3) by G^{-1}, we obtain an explicit expression for the angular spectrum on the surface of the source $z = 0$:

$$P(k_x, k_y, 0, \omega) = P(k_x, k_y, z_H, \omega) e^{-i\sqrt{\frac{\omega^2}{c^2} - k_x^2 - k_y^2} z_H}. \quad (5)$$

It should be noted here that for k_x, k_y values outside a circle with radius ω/c, the power of the exponent will be a positive real number, which with the inevitable noise introduced into the function $P(k_x, k_y, z_H, \omega)$ in holographic measurements will lead to an exponential increase in errors in determining the initial field. Therefore, as noted above, in problems with large wave dimensions, inhomogeneous (evanescent) waves are mandatorily excluded from consideration, which in the angular spectrum method is carried out by using only spectral components in the limit of the so-called radiation circle $(k_x, k_y) \in \Sigma_k$, which is determined by the condition $(k_x, k_y) : k_x^2 + k_y^2 \le \omega^2/c^2$.

It is convenient to write the final expressions for calculating the initial field at the source using transformations inverse to (1), (2) and relation (5) $p(x, y, 0, t)$, based on the measured field along the plane surface of the hologram $p(x, y, z_H, t)$, which were used in this study:

$$p(x, y, 0, t) = \frac{1}{(2\pi)^3} \int_{-\infty}^{\infty} \left\{ \iint_{\Sigma_k} P(k_x, k_y, z_H, \omega) e^{-i\left(\omega t - k_x x - k_y y + \sqrt{\frac{\omega^2}{c^2} - k_x^2 - k_y^2} z_H\right)} dk_x dk_y \right\} d\omega, \quad (6)$$

where

$$P(k_x, k_y, z_H, \omega) = \iint_{-\infty}^{\infty} \left\{ \int_{-\infty}^{\infty} p(x, y, z_H, t) e^{i(\omega t - k_x x - k_y y)} dt \right\} dx dy. \quad (7)$$

As noted above, calculation of the field using the obtained formulas is possible only for plane-parallel surfaces. For real measurements, however, deviation of the transducer and hologram surfaces from the mutual parallelism is inevitable [16], which formally makes the proposed method not directly applicable to real conditions. This, however, is not a serious problem, since even a monochromatic hologram is a set of data on the full three-dimensional spatial structure of the field in the region of interest, which means that even in the case of mutual nonparallelism of surfaces, information about the field along the required surface can be reconstructed with the angular spectrum method. For example, with linear deviations on the order of the wavelength on the transverse scale of the hologram, with the direct application of the method, the reconstruction error is a few percent [16]. In the case of large deviations or if it is necessary to correct the resulting larger error, it can be compensated by introducing additional phase factors in the transform (7), which was analyzed in [25].

EXPERIMENTAL

The proposed method was experimentally verified with a two-dimensional transceiver array of piezoelectric elements in the form of a plane square matrix (see Fig. 1). The matrix is square, planar, and 20 × 20 elements in size (with a total of 400 elements). The form of each matrix element is a square measuring 1.45 × 1.45 mm. The gap between adjacent elements is 0.05 mm (the matrix period is 1.5 mm). Of the 400 available elements, 384 are controlled (operational); divided into three groups A, B, and C with 128 elements each (the distribution of elements into groups is shown in Fig. 1b), each is controlled using a separate cable that connects to the output of a Verasonics system (the connector type conforms to Canon ZIF DL5-260PW6A).

The center frequency in transceiver mode for the minimum value of the reactive component of the impedance is in the range 1.9–2.3 MHz. The relative bandwidth in transceiver mode at a level of 6 dB with a minimum value of the reactive component of the

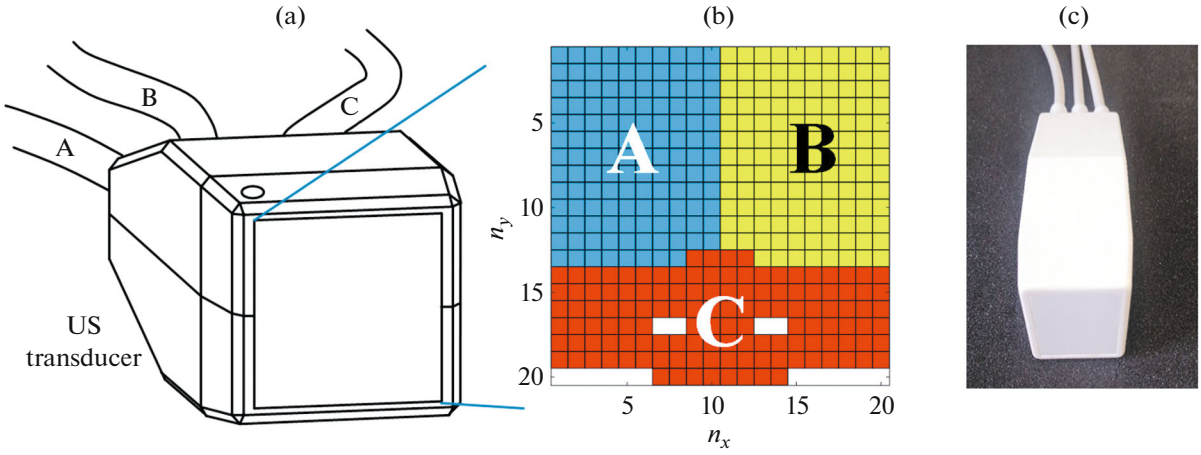

Fig. 1. (a, c) Two-dimensional ultrasonic transducer. Size of working area is 30 × 30 mm. (b) Layout of 384 active elements on front surface of sensor, divided into three sectors A, B, and C with 128 channels each.

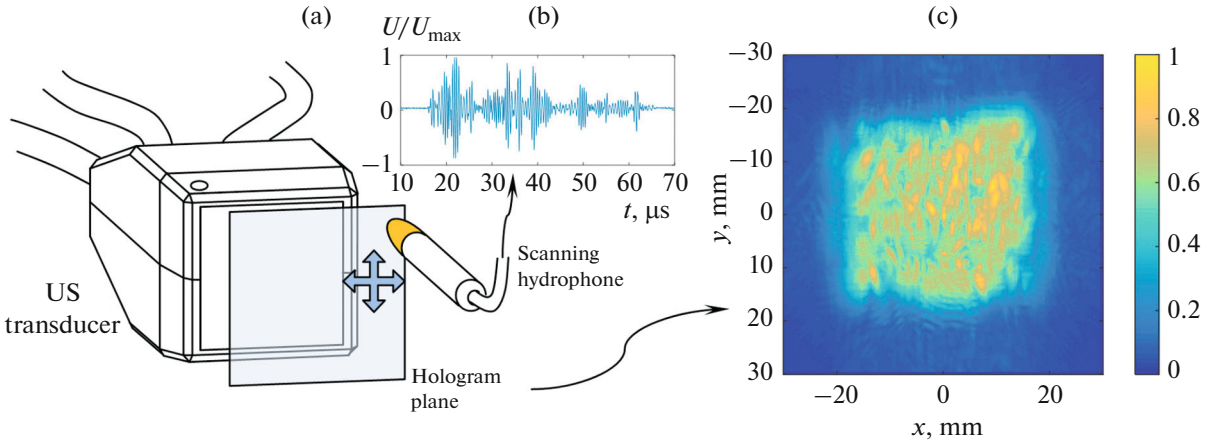

Fig. 2. (a) Measurements scheme with hydrophone moving along plane of hologram in front of the transducer at distance of 25 mm. (b) Typical temporal waveform of electric signal at hydrophone at one spatial point of hologram when source is excited in second mode (see text for explanation). (c) Distribution of electric signal peak values along hologram surface.

impedance is no less than 40%. The housing of the array with three compatible cables is waterproofed to provide immersion in water at room temperature to a depth of 1 m and remain under the specified conditions for up to 10 days.

Holographic measurements were carried out on a special experimental stand. The investigated ultrasonic array was immersed into a tank with degassed water and was fixed during measurements. In front of the transducer an ultrasonic sensor was located, a Golden Lipstick HGL-0200 capsule hydrophone (Onda Corp., USA) with a built-in electric signal preamplifier (Fig. 2a). The nominal diameter of the sensing area of the hydrophone is 0.2 mm; the sensitivity at a frequency of 2 MHz is 0.21 V/MPa.

During measurements, the hydrophone could be positioned in automatic mode. For this, a UMS-3 micropositioning system (Precision Acoustics, UK) was used, which allows 3D scanning with a step of 1 μm and a guaranteed positioning accuracy of 6 μm using a feedback system with magnetic linear encoders on each of the three axes.

The hologram of the ultrasound field was recorded via detection of the hydrophone signal at the nodes of a plane square grid with a resolution of 0.25 mm, oriented parallel to the radiating surface of the sensor at a distance of 25 mm from it. The corresponding number of grid nodes was chosen as 241 × 241; i.e., the size of the scanning area was 60.25 × 60.25 mm, which exceeded the transverse dimension of the ultrasound beam: the size of the working zone of the sensor was 30 × 30 mm with all elements excited. The center of the scanning area was established opposite the center of the ultrasonic sensor, which ensured almost com-

plete registration of the radiated acoustic beam within the scanning area.

The positioning system was located above a 1 × 0.5 × 0.5 m tank, which for measurements was filled with degassed filtered water. The tank walls were made of 12 mm plexiglass. Filtration, degassing, and bactericidal treatment (a UV lamp) was done with a water treatment system (Precision Acoustics, UK). The hydrophone signal was transmitted to an oscilloscope (TDS5054B, Tektronix Inc., USA) connected to a computer via a GPIB bus and a VISA virtual session via LAN. Centralized control of the measurement process was performed by computer using a program written in the LabView environment, which is part of the Precision Acoustics positioning system.

The signal was recorded within a time window of 100 μs. The specified duration was sufficient to record a pulsed acoustic signal recorded by the hydrophone. The hydrophone signal was recorded with a sampling step of 40 ns, which for the selected time window forms 2500 recording points. To reduce the noise level for each spatial point, averaging over 32 samplings of a periodically repeating signal was performed. Figure 2b shows a typical waveform of an electric signal recorded by the hydrophone at one of the points of the hologram plane during pulsed excitation of the ultrasonic array elements (a 60 μs window containing a signal is shown).

The investigated transducer was connected to two Verasonics V-1 systems (Verasonics Inc., USA) with the ability to control 256 channels each. Two groups of array elements A and B (Figs. 1a, 1b) were connected by two connectors to the first Verasonics system, and group of elements C was connected by a third connector to the second Verasonics system. Two modes were used. In the first mode, all sensor elements were excited synchronously by the same signals, representing three electric voltage periods in the form of a meander with a frequency of 2 MHz and a peak voltage of 10 V. In the second mode, the elements of the three groups were excited by the same signals, but with a delay of $(n-1)\cdot 392$ ns, where n is the number of the output channel of the Verasonics system within the range 1–128 for each of the three groups. The two systems were synchronized with an external generator (Agilent 33250A, Agilent Technologies, USA). These pulsed signals were periodically repeated at a frequency of 100 Hz.

The measurement result was a transient hologram, which was a set of 58 081 records of the time profile of the hydrophone signal in various positions corresponding to the nodes of a measurement grid with a size of 241 × 241. The typical distribution of peak values on the plane of the hologram in the second mode (within a time window of 100 μs for each spatial position) is shown in Fig. 2c. Based on these data, using the backpropagation algorithm in accordance with the above-described method (6)–(7), the procedure for reconstructing the distribution of oscillations of the surface of the sensor under study was carried out. As a result, the distributions of the time dependence of the acoustic pressure and normal component of the vibrational velocity on the surface of the array were found. By calculating the spectra of the indicated dependences, we also found the spatial distributions of the signal amplitudes corresponding to the vibrations of the array surface under continuous (harmonic) excitation at different frequencies within the effective radiation band of the sensor.

In addition to hydrophone measurements, echo pulse measurements were carried out for each element of the array. For this, one sector of elements A, B or C was connected to the Verasonics V-1 system, for which an emission protocol was formed using the above-described signal to excite only one element of the connected 128-element group. The signal was emitted into water, where at a distance of 50 mm the plane surface of a brass block was located, parallel to the transducer surface. The signal reflected from the surface of the block fell back on the surface of the transducer, after which it was recorded by 128 channels of the receiving path of the ultrasound system connected to the current group of elements. Recording signals from all elements of this group, not just the emitting one, made it possible to identify elements electrically closed to each other, operating in parallel. Initially, these measurements were carried out in order to compare the sensitivity distributions of the elements in the transceiver with the distribution obtained as a result of holographic reconstruction, which corresponds to the sensitivity distribution in the emitting mode. As it turned out, there was a discrepancy in the table of pin connections to the transducer elements, which did not allow for a correct comparison of the distributions. The use of the second emitting mode (see above), together with measurement of the hologram, made it possible to establish the correct channel number–element relationship for all 384 active elements.

At the final stage, as an additional control of the obtained distributions, the electric capacitance of all active elements with supplied cables was measured. This was done with a digital RLC E7-8 meter at the contacts of the connectors in accordance with the established connection of the connector contacts with the piezoelectric elements of each group.

RESULTS AND DISCUSSION

According to the described method, the field on the transducer surface was reconstructed from the measured holograms (Figs. 2b, 2c). The angular spectrum for each spectral band (when expanded in time harmonics) was calculated numerically using expression (7), where the integral Fourier transforms were replaced by a set of fast Fourier transform (FFT) operations. In some cases, before the transformations, the spatiotemporal calculation domain was supplemented

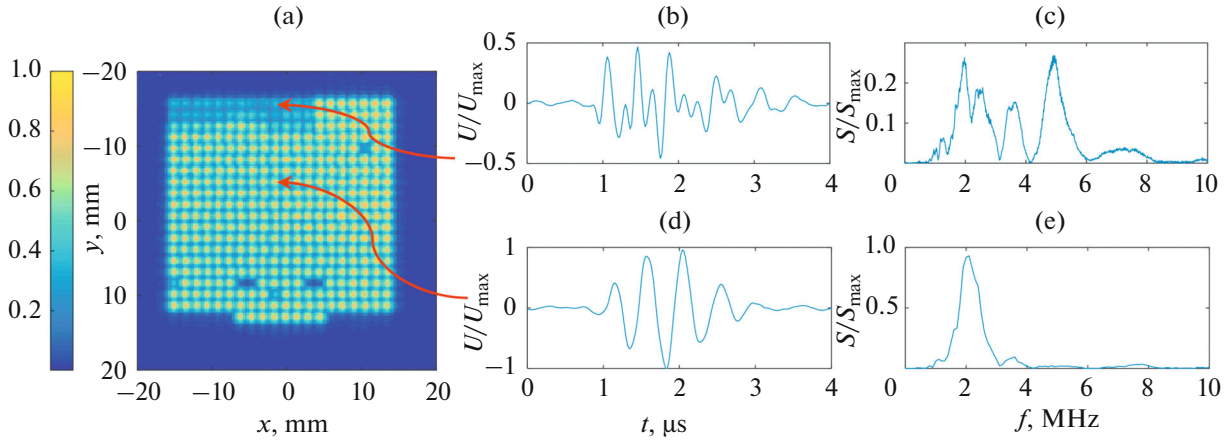

Fig. 3. (a) Normalized distribution of peak field values on surface of transducer, calculated from hologram in Fig. 2c. Time profiles of signal at centers of source elements indicated by arrows: from (b) defective and (d) normal regions; (c, e) corresponding frequency spectra.

with zeros to avoid spectral overlap. The algorithm for numerical calculation of the field on the transducer surface was realized in the MATLAB environment. Based on the results of calculating the field on the surface of the source, distributions were obtained for the two radiation modes described above: in-phase and sequential excitation of the transducer elements. Figure 3 shows the result of reconstructing the field on the transducer surface operating in the second mode. On the left, the two-dimensional distribution of acoustic pressure peaks is shown, normalized to a maximum in a given plane. In this radiation mode, all piezoelectric elements distinctly differ, in particular, the inactive elements and differences in the level of radiation of active elements.

At the edge of the working surface, in the area of zones A and partly B, there is a clearly defined defective area, which affects about 40 elements of the array. Within this section, in the operating frequency range of 1–3 MHz, element vibrations are almost completely suppressed compared to all other active elements. To analyze the nature of element vibrations (indicated by arrows in Fig. 3a) from the composition of the defective and normal regions in Figs. 3b, 3d show the time profiles of the emitted signals. It is clearly seen that the overall signal level at the element of the defective area is much lower and the structure of the oscillations has an irregular shape. When considering the spectral composition of the signals (Figs. 3c, 3d), a significant peak in the 5 MHz region is noticeable, which is absent in the elements of the normal region.

It is useful to illustrate the distribution obtained on the surface of the source, not in the form of the two-dimensional pattern of the signal peak values, like in Fig. 3, but in the form of a set of monochromatic holograms corresponding to the distribution of the actual amplitude of the acoustic pressure created by the surface of the source in water for the selected spectral components. Fig. 4 shows such holograms for frequencies from 1 to 9 MHz with a step of 1 MHz for the in-phase radiation mode with all elements. It should be noted that the presented set is only a small part of the entire transient hologram, which usually consists of several thousand spectral components (5000 components for the presented transient hologram). In this case, in contrast to the radiation mode with sequential excitation (Fig. 3a), individual elements within the working zone are not so distinguishable, which is clearly seen in the distribution for a center frequency of 2 MHz (Fig. 4). This is due to the fact that in the mode of in-phase excitation, the entire surface of the source, together with the matching layer and gaps between elements filled with compound, vibrates as a single piezocomposite plate, while for sequential excitation of the elements, the active region of radiation is localized in the area bounded by the oscillating element, with an almost zero level in areas between elements. In this case, a comparison is made between the distribution of the peak values of the signal time profiles (Fig. 3a) and the distribution of the spectral component (2 MHz in Fig. 4), which, strictly speaking, is incorrect, but useful for illustrating the difference between the two radiation modes, since the distribution of the spectral component at the center frequency of 2 MHz corresponding to the one in Fig. 3a will visually repeat it.

The representation of a transient hologram as a set of monochromatic holograms (Fig. 4) makes it possible to analyze the behavior of the defective region in comparison to the other elements at different frequencies, which is often more convenient than a spatiotemporal representation (Fig. 3). Thus, it is clearly seen that in the fundamental frequency band of about 2 MHz, the defective region hardly radiates, while in the high frequency range (5, 6, 7 MHz in Fig. 4) it radiates much more effective than the other elements.

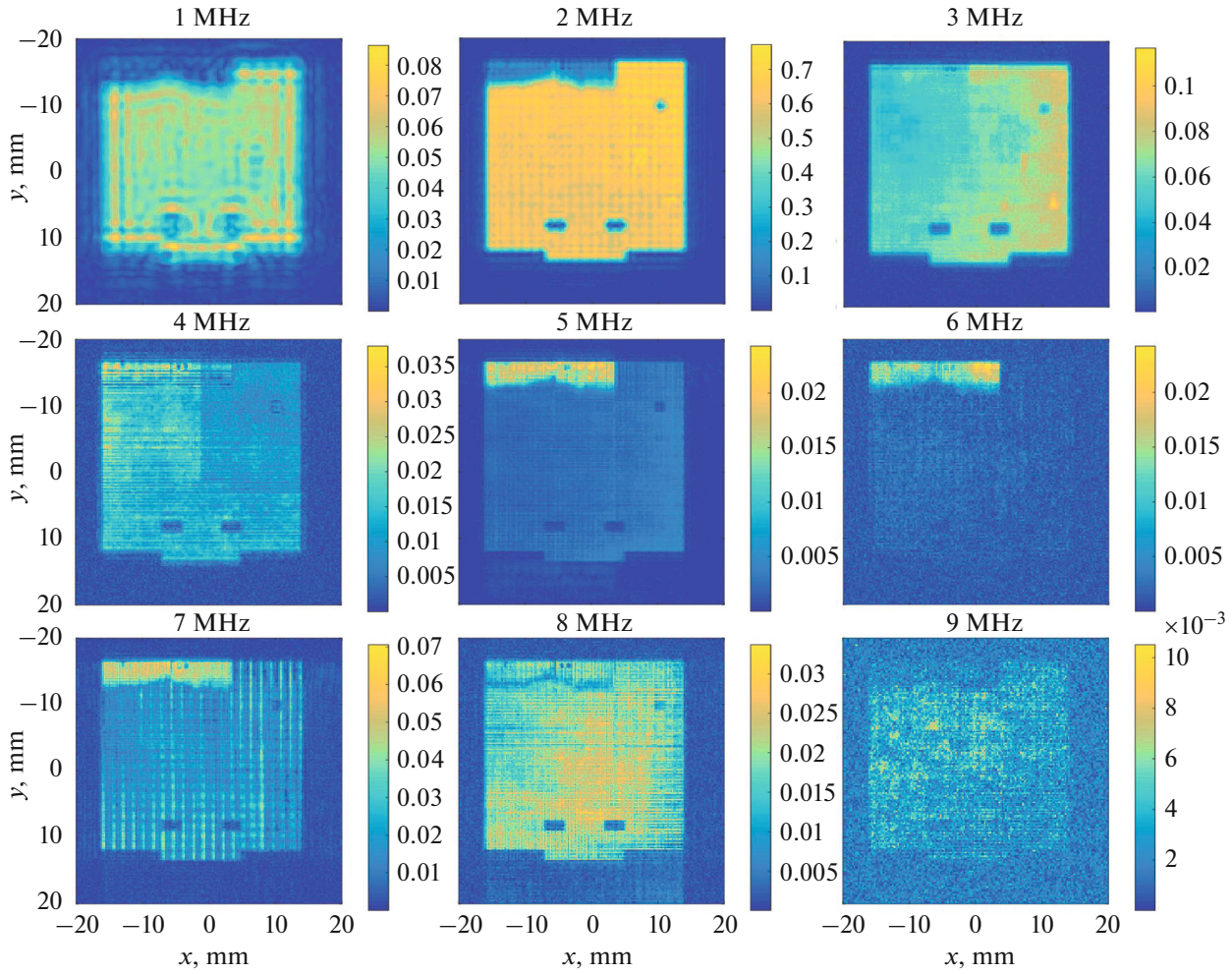

Fig. 4. Distributions of real field amplitudes on surface of source for monochromatic components in range of 1–9 MHz with step of 1 MHz, calculated from hologram for mode with in-phase radiation by all elements. Defective area of elements is clearly visible, which does not radiate at fundamental frequency, but operates at frequency of 5 MHz. Normalization of color scale is uniform for absolute maximum of the field in the plane among all frequencies.

At a frequency of 8 MHz, a boundary between the defective and working areas can be noted.

To control the distributions obtained from the hologram, elementwise echo pulse measurements with reflection from a brass block in water were carried out (Fig. 5a), as well as measurements of the electric capacitance of the elements, the technique of which is described in the previous section. Figure 5b shows the results of echo pulse measurements using the supplied channel wiring circuit for the elements attached to the transducer. The structure of the distribution of electric capacity had a similar structure and is not presented here. Due to the irregular structure of the obtained distributions, it was decided to compare the channel numbers with the corresponding elements using the second radiation mode with sequential excitation of the elements. For this, the hologram was measured; the field on the surface of the source was reconstructed in the time representation and the time points at which only one element within each sector A, B, and C radiated were selected. The channel number active at that moment was chosen from the radiation protocol and was assigned to the active element on the hologram of the surface of the source. Thus, a new diagram of the correspondence of the channel and piezoelectric elements was determined, according to which the sensitivity distribution in the echo pulse mode corresponding to the real one was constructed (Fig. 5c). For convenience of comparison, the resulting distributions are shown in Fig. 6. There is good agreement between the field structure on the surface of the source at the center frequency (Fig. 6a), the sensitivity distribution of the elements in the echo pulse mode (Fig. 6b), and the electric capacitance distribution of the elements with the supply cable and connector (Fig. 6). On all three distributions, the elements of the defective area are highlighted against the elements of the working area.

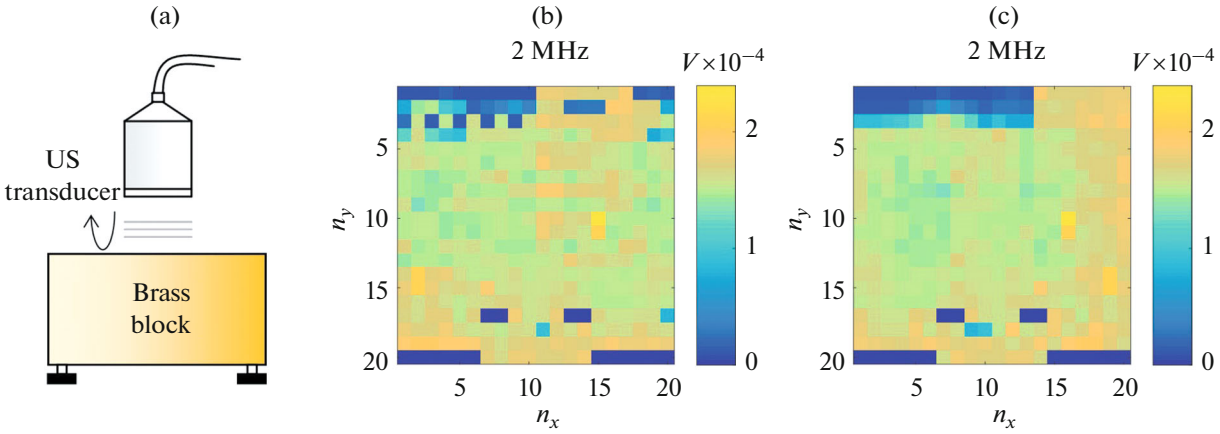

Fig. 5. (a) Measurement scheme for determining relative sensitivity of elements by echo pulse method. Amplitude distribution of received echo signal over sensor surface: (b) for use of supplied layout of correspondence between channel number and position of element; (c) for determination of correspondence by transient holography method.

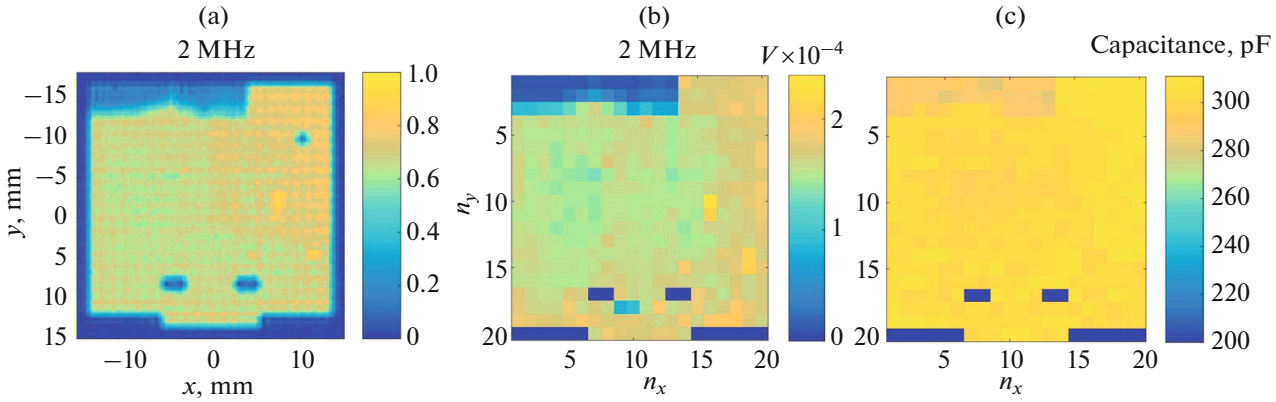

Fig. 6. Comparison of distributions based on results of: (a) holographic reconstruction of field on surface of two-dimensional array for frequency of 2 MHz in in-phase radiation mode (see text); (b) elementwise echo pulse measurements using brass block at frequency of 2 MHz; (c) elementwise electric capacitance measurements.

The specified defect was most likely unrelated to any problems with the electric connection. It seems to have been cause by mechanical reasons, since (a) the lower boundary of the defective area is uneven and does not pass along the line of separation of elements and (b) the defective area affects two groups of elements (A and B), which are connected by different connectors of the Verasonics system. This defect is most likely not delamination between the matching layers, since, as already noted, in the frequency range of 3.7–7 MHz, this are, on the contrary, radiates well, while the rest of the region is suppressed. The probable cause of the defect may be a thickness of the matching layers at this spot differing from nominal.

It should be noted that in the areas of the surface outside the defective area, the vibrations of various elements are identical with high accuracy, except for certain small areas. A single inactive element, clearly visible in sector B at the center frequency (Fig. 6a), is associated with a defect in the radiating channel of the second Verasonics system, since when this sector is connected to the first connector of the other system (Fig. 6b), the element becomes active; the integrity of the cable and absence of problems with the contact of the element are also confirmed by the almost uniform level of the electric capacitance (Fig. 6).

CONCLUSIONS

The article shows the possibility of using transient acoustic holography to determine the nature of surface vibrations of a multielement two-dimensional ultrasound array in order to detect defects and calibrate according to the level of the radiated field in different modes. It is also shown that the method can be used to identify the scheme of correspondence between the channel number of the radiating system and position

of the element on the surface of the transducer, which can be very useful in the absence of a factory scheme. It is shown that the results obtained using the transient acoustic holography method are in good agreement with the results of independent elementwise echo pulse and electric capacitance measurements.

The method is very promising for characterizing virtually any ultrasound transducers operating in complex modes, making it possible to obtain quantitative spatiotemporal distributions not only on the surface of the source, but also in any region within the accuracy limits of the method [16].

FUNDING

The study was supported by a grant from the Russian Science Foundation (no. 14-12-00148).

ACKNOWLEDGMENTS

The authors are grateful to I.V. Movshovich for discussion of the technical characteristics of the studied ultrasonic array.

REFERENCES

1. S. Ting, Z. Shi, L. Dayu, and Y. Dingjie, Acoust. Phys. **64** (3), 379 (2018).
2. W. Ping, S. Yizhe, J. Jinyang, K. Lu, and G. Zhihui, Acoust. Phys. **65** (1), 123 (2019).
3. E. G. Bazulin and D. M. Sokolov, Acoust. Phys. **65** (4), 432 (2019).
4. S. A. Titov and P. V. Zinin, Acoust. Phys. **66** (2), 198 (2020).
5. P. B. Rosnitskiy, O. A. Sapozhnikov, L. R. Gavrilov, and V. A. Khokhlova, Acoust. Phys. **66** (4), 352 (2020).
6. D. Cathignol, O. A. Sapozhnikov, and J. Zhang, J. Acoust. Soc. Am. **101** (3), 1286 (1997).
7. N. A. Halliwell, in *Laser Vibrometry Optical Methods in Engineering Metrology,* Ed. by D. C. Williams (Chapman and Hall, London, 1993), Chap. 6, p. 179.
8. O. A. Sapozhnikov and M. A. Smagin, Acoust. Phys. **61** (2), 181 (2015).
9. W. A. Riley and W. R. Klein, J. Acoust. Soc. Am. **42** (6), 1258 (1967).
10. O. A. Sapozhnikov, A. V. Morozov, and D. Cathignol, Acoust. Phys. **55** (3), 365 (2009).
11. O. A. Sapozhnikov, A. E. Ponomarev, and M. A. Smagin, Acoust. Phys. **52** (3), 324 (2006).
12. *Acoustical Holography* (Sudostroenie, Leningrad, 1975), p. 304 [in Russian].
13. L. D. Gik, *Acoustical Holography* (Nauka, Novosibirsk, 1981) [in Russian].
14. A. I. Malyarovskii, V. I. Pronyushkin, and Yu. V. Pyl'nov, in *Scientific Works of Prokhorov General Physics Institute of the Russian Academy of Sciences "Optoelectronic Processing of Remote Sensing Data"* (1990), **Vol. 22**, p. 78.
15. O. A. Sapozhnikov, Yu. A. Pishchal'nikov, and A. V. Morozov, Acoust. Phys. **49** (3), 354 (2003).
16. O. A. Sapozhnikov, S. A. Tsysar, V. A. Khokhlova, and W. Kreider, J. Acoust. Soc. Am. **138** (3), 1515 (2015).
17. D. A. Nikolaev, S. A. Tsysar, V. A. Khokhlova, W. Kreider, and O. A. Sapozhnikov, J. Acoust. Soc. Am. **149** (1), 386 (2021).
18. M. Forbes, S. V. Letcher, and P. R. Stepanishen, J. Acoust. Soc. Am. **90**, 2782 (1991).
19. C. J. Vecchio and P. A. Lewin, J. Acoust. Soc. Am. **95** (5), 2399 (1994).
20. P. R. Stepanishen and K. S. Benjamin, J. Acoust. Soc. Am. **71**, 803 (1982).
21. E. G. Williams, *Fourier Acoustics: Sound Radiation and NAH* (Academic, London, 1999).
22. S. A. Tsysar, Y. D. Sinel'nikov, and O. A. Sapozhnikov, Acoust. Phys. **57** (1), 94 (2011).
23. E. G. Williams and J. D. Maynard, Phys. Rev. Lett. **45**, 554 (1980).
24. M. Fink, Phys. Today **50** (3), 34 (1997).
25. S. A. Tsysar', O. A. Sapozhnikov, S. N. Gurbatov, I. Yu. Demin, and N. V. Pronchatov-Rubtsov, Vestn. Nizhegorod. Univ. im. N. I. Lobachevskogo **3** (1), 230 (2013).